Environmental Earth Sciences (2024) 83:133
https://doi.org/10.1007/s12665-023-11383-3

ORIGINAL ARTICLE

Assessing the influence of climate variability and land cover change on water resources in the Wami river catchment, Tanzania

Christossy B. C. Lalika[1] · Aziz Ul Haq Mujahid[2] · Makarius C. S. Lalika[1,3]

Received: 5 July 2023 / Accepted: 22 December 2023

Abstract

Understanding the trend, extent, and effect of climate variability and land cover change are globally important for monitoring river catchments water resources. Due to the majority of river catchment from developing countries such as Tanzania experiencing insufficient time series data, the long-term ERA5-Land (1960–2021) reanalysis was used to assess the influence of climate variability and land cover change on water resource in the Wami river catchment. The Mann–Kendal–Sneyer test revealed a change that reflects the effect of land cover change on runoff in 1992, hence the mean annual runoff, precipitation, and actual evapotranspiration decreased by 19%, 9.7%, and 8.9%, respectively, while potential evapotranspiration increased by 5% after the change. Budyko decomposition and climate elasticity methods illustrated that variability change caused a notable contribution to the reduction of Wami River runoff. Hydrological sensitivity analysis revealed that variability of climate is a primary factor that reduced runoff with a contribution of 69%, while land cover change is 31%, this illustrates runoff in the Wami river catchment is more vulnerable to climate variability than land cover change by considering that most of the catchment are classified as arid or semi-arid. Thus, our study emphasizes the importance embracing climate adaptation strategies, particularly a nature-based solution (NbS), to ensure the sustainability of water resources within the Wami river catchment.

Keywords Climate variability · Land cover change · Runoff · Water availability · Wami river catchment · Remote sensing

Introduction

Across the globe, river catchments are vigorous systems that undergo complex process caused by climate, physical properties of catchment, and anthropogenic actions (Dey and Mishra 2017). These process are being affected by climate change and anthropogenic operations, which is leading to a decrease in water resources and an increase in the number of hydrological disasters (Chen et al. 2013). The alteration in precipitation and temperature are the driving force behind these changes, and they are being accelerated by global warming. Anthropogenic activities are also influencing runoff variability, as a results of land use and land cover changes (Lang, et al. 2017; Balist et al. 2021).

Apart from climate change and variability, anthropogenic actions alter land use land cover (LULC) changes, and hydrologic processes which eventually significantly affect ecosystem types and services, landscape patterns and ecological processes, ecosystems diversity, river catchments, and water resources (Balist et al. 2021). Therefore, considering the aforementioned factors of increasing water use,

✉ Christossy B. C. Lalika
christossylalika@gmail.com

Aziz Ul Haq Mujahid
haq753@gmail.com

Makarius C. S. Lalika
makarius.lalika@yahoo.com

[1] UNESCO Chair on Ecohydrology and Transboundary Water Management, Sokoine University of Agriculture, P.O. Box 3038, Morogoro, Tanzania

[2] Swiss Federal Institute of Technology, ETH Zurich, Zurich, Switzerland

[3] UNESCO Chair on Ecohydrology and Transboundary Water Management, Department of Geography and Environmental Studies, College of Natural and Applied Sciences, Sokoine University of Agriculture, P.O. Box 3038, Morogoro, Tanzania

Published online: 13 February 2024

climate change, and LULC changes, achieving sustainable water resources at a catchment becomes exceedingly challenging (Kim et al. 2014; Shao et al. 2019). Quantifying the effects of climate change on water resources is important for the sustainability of river catchment management for the current and future generations. This is because climate change is already having a significant impact on river catchments, as evidenced by the reduction of 17% in stream flow in several major rivers catchment in Tanzania (Lalika et al. 2015). The primary cause of this reduction is the alterations in precipitation and temperature, both stemming from the climate change. The impact of climate change and anthropogenic actions is more significant in arid and semi-arid areas, resulting in changes in water resources (Chen et al. 2013). This is also true for the Wami/Ruvu catchments, which are largely arid and semi-arid and have experienced changes in both climate and LULC which cause the decline of water availability within the catchment (Wambura et al. 2015). The population of the Wami/Ruvu river basin is estimated to be 10 million according to 2019 estimates (Twisa and Buchroithner 2019; Kanyabwoya 2022).

The impact of climate change and land cover change on water resources is a complex issue, and the severity of these impacts in the Wami river catchment has not been fully quantified. However, there is evidence that these impacts are already having a negative impact on the availability of water for both human and environmental use (Kalugendo 2014). A recent article published in The Citizen newspaper on 11th November 2021, described a water shortage in Dar es Salaam. The city relies on water supplies from the Wami River and Upper Ruvu River, but these rivers have been experiencing a reduction in water level due to drought (Nachilongo 2021).

The lack of accurate ground-based data in the Wami river catchment has made it difficult to assess the impact of climate change and anthropogenic actions on water resources. Ground stations are inadequate and unevenly distributed globally and in most low-income countries (Ayehu et al. 2017). Wami river catchment is also among the catchment in Tanzania, facing the challenge of lacking in-situ measured data (Mulungu and Mukama 2022). In recent years, there have been significant advances in remote sensing, reanalysis, and machine learning, weather data from satellites has become an alternative data source, reducing the big gap of unavailability of accurate ground-based data sets (Nawaz et al. 2021). Despite advancement in remote sensing RS, reanalysis data are widely used due to its ability to produce consistent time series of various climatic variables. This is achieved by employing the latest model and incorporating up-to-date global observations (Chiaravalloti et al. 2022). To address the challenges of obtaining accurate ground-based data, the used ERA5-Land reanalysis data were applied. The ERA5-Land is a global product produced by the European Centre for Medium-Range Weather Forecast (ECMWF) as part of the 5th generation of European Reanalysis (ERA5) (Dhawan et al. 2023). This data source was chosen as it offers a wide range selection (i.e., a total of 50) of weather parameters, and enhances the robustness and scope of our research findings. The ERA5-Land data set offers hourly temporal resolution, incorporating surface modelling (H-TESSEL), an advanced 4D-var data assimilation scheme, and a numerical weather prediction model shared with ERA5 (Muñoz-Sabater et al. 2021; Xie et al. 2022). As a result, it provides a spatial resolution of 9 km, enhancing the precision and accuracy of the data (Xie et al. 2022).

The ERA5-Land reanalysis data are a valuable resource of data that can be used to improve our understanding of the impact of climate change and anthropogenic actions on water resources in the Wami river catchment. By assessing the potential causes of these changes, could help to improve understanding of hydrological variation, develop sustainable river catchment management strategies, and help decision-makers develop sustainable solutions to tackle the challenges of water scarcity and adaptation to climate change.

Materials and methods

Description of the study area

This study took place within the Wami river catchment, located in the eastern-central area of Tanzania between latitude 5° 00–7° 27′ S and longitude 36° 00′–39° 00 E (Fig. 1). The catchment consists of an area of 43,743 km^2 that is divided into three sub-catchments, namely, Kinyasungwe (16,509 km^2), Mkondoa (12,964 km^2), and Wami (14,270 km^2). However, in this study, a total area of 41,073 km^2 was used by considering hydrological stations as a benchmark point. Dodoma Region forms a large part of the catchment and is a plateau, while the Uluguru and Udzungwa Mountains in Morogoro Region form the roof part of the basin. The elevation of the Wami River sub-basin ranges from 0 to 2382 m. The catchment has an average rainfall of 550–1000 mm per annum (Ngondo et al. 2022). The study area consists of distinct rainfall seasons, which are unimodal rainfall occurring from December to May in the western and southwestern parts. In addition, bimodal season, occurring in eastern and northeastern parts as these regions experience two wet periods between October to December, and March and May (Luhunga 2018). The mean annual temperature within the area ranges from 12 to 24 °C (Wambura et al. 2015).

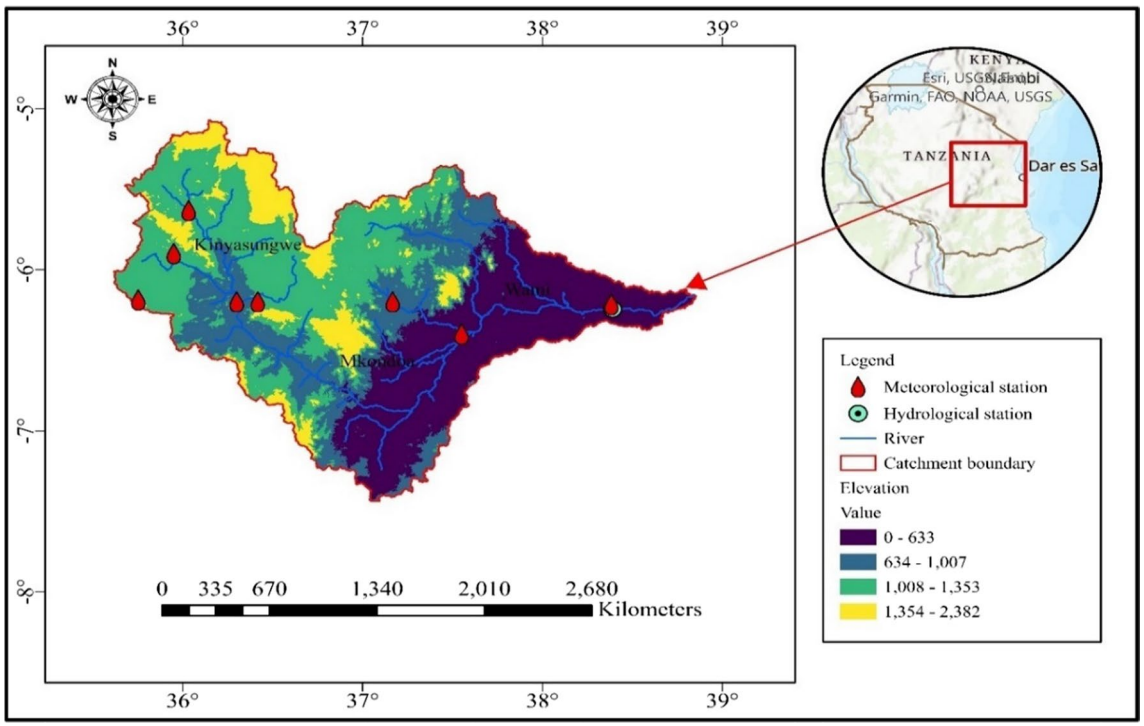

Fig. 1 Wami river catchment

Data sources

Landsat satellite imagery acquisitions, processing, and classification

The Landsat imageries have been used to analyse Land use/cover (LULC) changing patterns throughout the Wami river catchment and are in four different paths and rows of Landsat images tiles (such as paths, 166,167,168 and rows 66, 65) with 30 m of spatial resolution as indicated in Table A.1 in the supplementary material. To cover the entire area, six Landsat data sets for each year were obtained from the United States Geological Survey (USGS) Earth Explorer website https://earthexplorer.usgs.gov/, and thus 16 cloud-free images were acquired by considering dry season (June–August) to minimize seasonal influence. Using radiometric calibration and dark subtraction, fast line of sight atmospheric analysis of spectral hypercube (FLAASH) was used to atmospherically correct each image scene in the ENVI 5.3 software (produced by Hariss Geospatial Solutions in Broomfield, Colorado, USA) (Ngondo et al. 2021). The top of atmosphere (TOA) reflectance was obtained using the Landsat digital numbers (DNs). The adjusted Landsat images were then mosaicked into a single composite image and clipped to research area boundary. This study was conducted for 30 years, using decade intervals (1991, 2001, 2011, and 2021). In addition to satellite images, several reference data sets were acquired, including topographical data such as a digital elevation model and a Google Earth image for accuracy assessment of the classification of land use land cover change and a total of 450 ground truth were collected using google earth to assist in the accuracy assessment process of the study area.

Seven major classes of land use land cover were identified which are forest, agriculture land, bare-land, bushland, woodland, built up area and wetland, as outlined in Table 1. To develop accurate result of classification from Landsat images we applied an integrated image classification method which involves combination of both spectral bands and various indexes approach. Random forest supervised classifier was used in this study to digitally categorize Landsat images into various classes of land use/cover. Random forest algorithm is non-parametric and Ensemble learning algorithms which have recently increasing interest in use in remote sensing, because they are more accurate and robust to noise than single classifiers (Dietterich 2000; Belgiu and Drăguţ 2016).Also, it is relatively robust to outliers and noise.

Accuracy assessment

Accuracy evaluation was purposely to evaluate the degree to which pixels have been correctly assigned to their respective land cover classes (Rwanga and Ndambuki 2017). Ground

Table 1 Land use/cover classes categories identified in the study area

Sn	LULC category	Description
1	Built up area	Urban settlements, Rural/Trading center, transportation networks, commercial and industrial area
2	Agriculture land	Agriculture fields
3	Bare land	Exposed field of land and sand fill area
4	Bush land	Shrubs, scrub and bushed
5	Woodland	Open Crown trees
6	Wetland	Covered with shallow water, Perennial water body, lake, ponds and other water reservoir, and flowing water confined in a channel
7	Forest	Evergreen and semi evergreens forest cover

truth techniques using field survey conducted from 01 august 2021 to September 15, 2021, for a total of 450 sample covering about 1750 km of road travel in the Wami river catchment. Ground data were collected based on pre-classified output, handheld Garmin GPS and Cannon Camera were used to capture information in the field. The ground point information was collected from 300 m × 300 m plots and capture GPS locations, land use/cover categories, and the estimate of land cover percentages. Ground point sample were acquired within large continuous of a particular land use/cover. Furthermore, Google earth pro was employed as additional ground survey information in class identification for previous years' land use/cover image generate.Confusion matrix table (error matrix) was generated with the use of Arc map 10.8 which is widely used in reporting the accuracy of classification obtained from remotely sensed data (Roy et al. 2015). This model of error provides the estimates for user, and producer accuracy along with the error of inclusion and exclusion and overall accuracy for each classification (Roy et al. 2015). Kappa statistic (Khat) is another accuracy approach used in this study and is used to measure the matrix agreement (Cohen 1960).

To assess the accuracy of LULC, a total of 480 ground truth sample points were generated using a random sampling approach in Google Earth. The accuracy assessment process was then performed in ArcMap (10.8.2) software using the class values. Finally, an error matrix table was created, which consists of different statistical measurements. The Kappa statistics, user accuracy, producer accuracy, and overall accuracy were calculated from the values in the matrix using the following formulas:

$$Overallaccuracy = \frac{sumofdiagonalelements}{Totalnoofaccuracysites(pixels)} \times 100 \quad (1)$$

$$KappaStatistics = \frac{Obs-exp}{1-exp} \quad (2)$$

where *Obs* represent accuracy found in the error matrix (overall accuracy) and *exp* represents correct classification. Based on the accuracy and classification, seven major LULC classes were identified as presented in Table A.2 in supplementary material. These classes include built-up, agricultural land, bare land, bushland, woodland, wetland, and forest (Fig. 2).

Climatological and hydrological data *Gauge data set*: Due to the scarcity of measured climate data sets in the study area, only available monthly meteorological data, specifically rainfall from a total of 8 weather stations (Fig. 1) were obtained. These stations were selected based on a reference period of 1991–2021 and the data were sourced from the Tanzania Meteorological Agency (TMA). It is evident as in Fig. 1 shows that the distribution of stations is quite spatial, with only eight available functioning stations covering an area of about 43,743 km^2. Only rainfall data from observed rain gauge stations were used to validate ERA5-Land precipitation within the catchment.

The standard normal homogeneity test (SNHT) (Alexandersson 1986) and Buishand's range test (1982) were used to evaluate the homogeneity of observed rainfall time series data at a 95% significance level. As Table 2 illustrates, all the observed rainfall data were found to be homogeneous.

ERA5-Land data set: The ERA5-Land is a reanalysis of the land surface variables that are based on the ECMWF, ERA5 climate reanalysis, and it has a native horizontal resolution of about 9 km, which means that it can capture smaller-scale features on the land surface (Chiaravalloti et al. 2022). Its coverage period is from 1950 to the present as it is illustrating in vast detail the water and energy cycles with hourly temporal frequency output (Muñoz-Sabater et al. 2021). The retrieved data at the monthly step used in this study are 2 m air temperature T (K), precipitation P (m), potential evapotranspiration PET (m), actual evapotranspiration AET (m), and surface runoff (m). The data were downloaded from the Climate Dara Store (CDC) https://cds.climate.copernicus.eu/ for the time interval from 1960 to 2021, whereby the store is a free and open-access repository of climate data.

Evaluation of observed rainfall and ERA5-Land precipitation: Several statistics metrics such as Pearson correlation

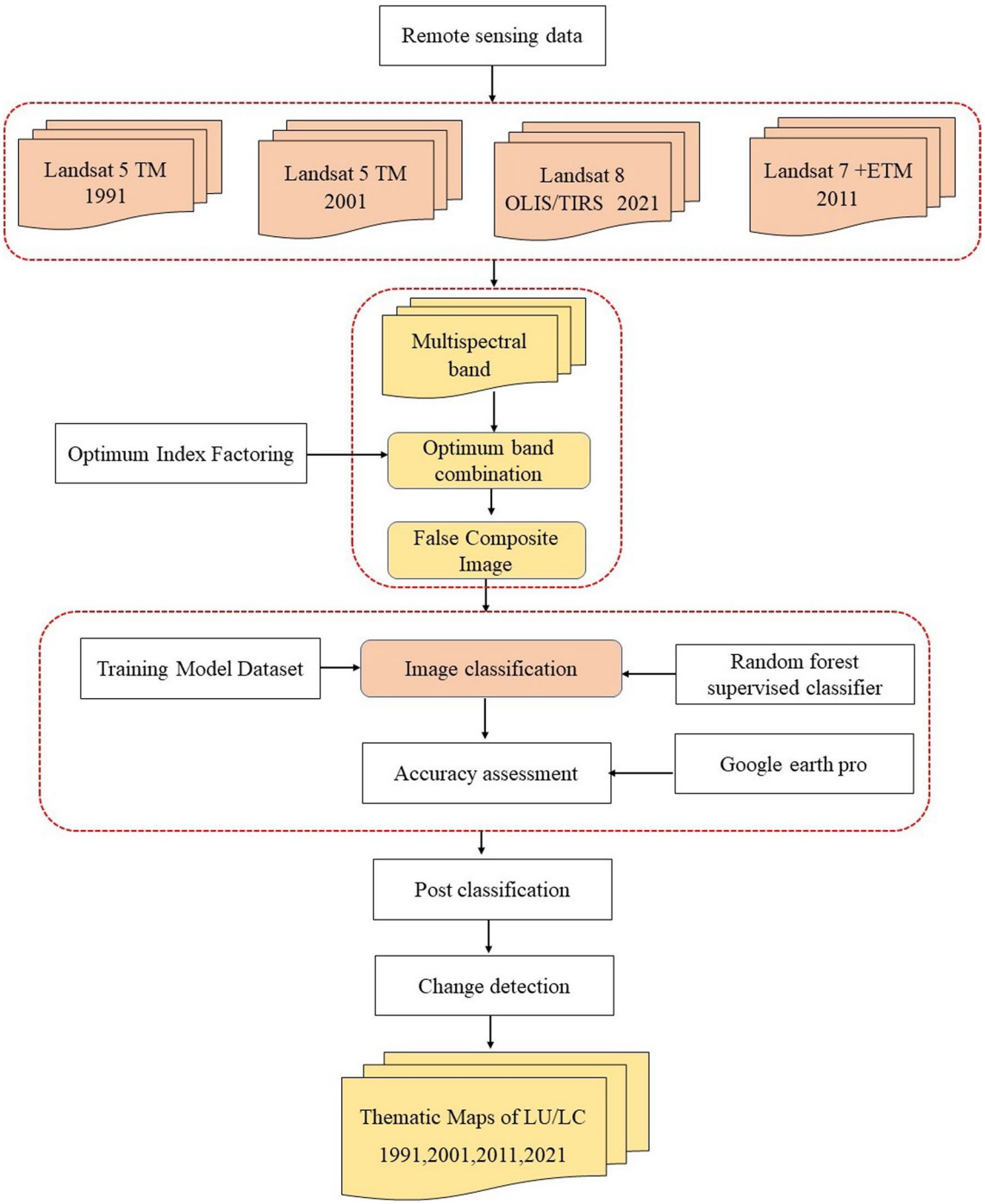

Fig. 2 Framework approach for the quantifying LULC in study area

(R), mean absolute error (MAE), root mean square error (RMSE), and percentage bias (PBIAS) for evaluating the performance of observed and ERA5-Land precipitation data (Xie et al. 2022) were used. The equations and optimal values are given in Table 3.

Whereby x_{ie} is the value of ERA5-Land data, y_{io} is observed data, $\overline{x}$ and $\overline{y}$ averages of observed and ERA5-Land precipitation, n is the degree of freedom of variables, and N is the total amount of data.

Mann–Kendall (MK) test The Mann–Kendall trend test is a non-parametric statistical that was found by Kendall and Mann (Mann 1945; Kendall 1975). It is a widely used method for identifying trends in hydro-climatological time

Table 2 Homogeneity results of observed rainfall series at 95% significance level

SN	Station name	Station ID	SNHT *P* value	BR *P* value
1	Barega	9,637,003	0.095	0.581
2	Dakawa	9,637,091	0.728	0.992
3	Dodoma	9,635,001	0.389	0.835
4	Hombolo	9,535,019	0.331	0.996
5	Itiso	9,536,002	0.471	0.877
6	Kinyasungwe	9,636,020	0.089	0.996
7	kongwa	9,636,029	0.077	0.967
8	Mandera	9,638,004	0.937	0.590

Table 3 Statistics indicators are used to evaluate the monthly observed and ERA5-Land precipitation

Statistics	Equations (3–6)	Range	Optimal value
R	$R = \frac{\sum_{i=1}^{n}(x_{ie}-\bar{x})(y_{io}-\bar{y})}{\sqrt{\sum_{i=1}^{n}(x_{ie}-\bar{x})^2}\sqrt{\sum_{i=1}^{n}(x_{io}-\bar{y})^2}}$	− 1 to 1	1
PBIAS	$PBIAS = \frac{\sum_{i=1}^{n}(y_{io}-x_{ie})}{N}$	$-\infty$ to ∞	0
RMSE	$RMSE = \sqrt{\frac{\sum_{i=1}^{n}(x_{ie}-y_{io})^2}{N}}$	0 to ∞	0
MAE	$MAE = \frac{\sum_{i=1}^{n}\lvert y_i-x_i\rvert}{N}$	0 to ∞	0

series data (Silva et al. 2015; Nyikadzino et al. 2020). In this study, the method was used to quantify the trends and magnitude of precipitation, temperature, PET, AET, and runoff change for the period from 1960 to 2021.

The MK test statistics (S) were computed using below equations:

$$S = \sum_{i=1}^{n-1}\sum_{j=i+1}^{n} sgn\left(\mathrm{X}_j - \mathrm{X}_\mathrm{i}\right) \quad (7)$$

whereby n indicated the number of observations, xi, and xj are the data values in time series which ranked as ith (i = i + 1……n) and jth (j = i + 1……n), respectively, of precipitation, temperature, and runoff. In addition, sgn $(\mathrm{X}_j - \chi_\mathrm{i})$ is signum function and computed as

$$sgn\left(\mathrm{X}_j - \chi_\mathrm{i}\right) = \left\{ +1 \ldots if\left(\mathrm{X}_j - \chi_\mathrm{i}\right) > 0, 0 \ldots if\left(\mathrm{X}_j - \chi_\mathrm{i}\right) = 0, -1 \ldots if < \left(\mathrm{X}_j - \chi_\mathrm{i}\right) < 1, \quad (8)$$

It has described that when n > 10, then statistics S is normally distributed with the mean E(S) = 0 (Eyasmin 2017), and its variance is computed using the following equation:

$$Var(S) = \frac{n(n-1)(2n+5) - \sum_{i=1}^{m} t_i(t-1)(2i+5)}{18} \quad (9)$$

whereby m = number of tied groups; (Σ) = summation of all tied groups, and $\mathrm{t_i}$ = the number of ith ties group (I = 1,2, 3….n). The presence of a statistically significant trend (i.e., standardized test statistics) $\mathrm{Z_c}$ is computed using Eq. (10), and formulated using S as follows:

$$Z_C = \left\{ \frac{S-1}{\sqrt{Var(S)}} \ldots ifS > 0, 0 \ldots ifS = 0 \frac{S+1}{\sqrt{Var(S)}} \ldots ifS < (0, \# \right. \quad (10)$$

The statistical trend was computed using the $\mathrm{Z_c}$ value. A positive value of $\mathrm{Z_c}$ indicates an upward, and a negative indicates a downward trend (Perera et al. 2020). The statistic $\mathrm{Z_c}$ has a normal distribution to test for either an upward or downward trend at α level of significance (usually 5% ± $\mathrm{Z_1}$-α/2 = 1.96) (Perera et al. 2020; Gocic and Trajkovic 2013).

Sen's slope estimator Sen's slope estimator was used to indicate the magnitude of the trend in the pair data set, and it is estimated using a simple nonparametric procedure developed by Sen, (Sen 1968). The slope is given by the following formula:

$$d_k = \frac{\mathrm{X}_h - \mathrm{X}_p}{h-p}, forp = 1, 2, 3 \ldots ., n \quad (11)$$

whereby $\mathrm{X_h}$ and $\mathrm{X_p}$ were considered as values at time j and k (j > k) correspondingly. The median of these *N* values of $\mathrm{Q_i}$ can be determined by Atta-ur-Rahman and Dawood (2017) and is represented as Sen's estimator of slope which is given as

$$\beta = \begin{cases} \mathrm{d}_{\frac{n+1}{2}}, nisodd, \\ \frac{1}{2}\left(\mathrm{d}_{\frac{n}{2}+}, \mathrm{d}_{\frac{n+2}{2}}\right), niseven \end{cases} \quad (12)$$

whereby the positive value of β illustrates an increase in trend, while the negative value of β showcases a decreasing trend, and zero illustrates no trend (Atta-ur-Rahman and Dawood 2017; Mohammad et al. 2022). As the value of β indicates the trend of data, Figure A.1 in supplementary material indicated variability in potential evapotranspiration, actual evapotranspiration, and temperature of the Wami river catchment from 1960 to 2021.

Identification of change point The Mann–Kendall–Sneyer test is a non-parametric method that was developed by Sneyers (1975). The method is commonly applied to detect the change point in the time series (Aminikhang-

hahi and Cook 2017). The test statistics were determined using the following formula:

$$S_x = \sum_{i=1}^{x} ri(2 \le x \le n \tag{13}$$

The test statistics are normally distributed with mean, and variance is given by

$$E_{Sx} = \frac{x(x-1)}{4} \tag{14}$$

$$var_{Sx} = \frac{x(x-1)(2x+5)}{72} \tag{15}$$

Let

$$Ufx = \frac{S_x - E_{Sx}}{\sqrt{var_{Sx}}}\# \tag{16}$$

whereby ufx is the forward, and the backward sequence ubx is calculated using the same equation but with reversed data (Ervinia et al. 2017).

ERA5-Land runoff data were used to detect the step change point in the Wami River runoff spanning from 1960 to 2021. When the intersection appears within the significance level, it signifies the presence of a step change point, as described by Chen et al. (2013). In this study, the curve intersection demonstrated a change in 1992 at the significance level of 0.05. Therefore, the study period was divided into two distinct periods: the pre-transformation period (1960–1992) and the post-transformation period (1993–2021). In the pre-transformation period, it was assumed that the variability in the catchment was solely influenced by climate change. Conversely, during the post-change, it was posited that the variability was influenced by both climate change and land cover change such as LULC in water resources within the catchment.

Conceptual approach *Tomer and Schilling's conceptual approach*: A conceptual method introduced by Tomer and Schilling, (Tomer and Schilling 2009), describes the utilization of water and energy within the catchment ecosystem. In addition, the approach emphasizes that alteration in the ecosystem is caused by shifts in climate, vegetation, or management practices, which can be reflected by changes in water excess (P_{ex}) and energy excess (E_{ex}) (Krajewski et al. 2021). This approach considers PET, AET, and precipitation to describe changes occurring in the particular catchment. The approach is written by the following formula:

$$E_{ex} = \frac{PE - AET}{PE}\# \tag{17}$$

$$P_{ex} = \frac{P - AET}{P}\# \tag{18}$$

Nevertheless, this method merely offers broad insights into whether the variation occurred due to climate change or anthropogenic actions (Dey and Mishra 2017).

Decomposition of the Budyko hypothesis To quantitatively examine the influence of climate variability and land cover change on the Wami River runoff, the hydroclimatic data set was subjected to the application of the Budyko model (Budyko 1948). This model characterizes the long-term water-energy balance within the catchment by taking into account the relationship between water and land heat balance (Liu et al. 2023). Therefore, the Budyko curve is written as follows:

$$\frac{AET}{P} = f\left(\frac{PET}{P}, basinproperties\right)\# \tag{19}$$

However, Krajewski et al., (2021) have illustrated that the aforementioned equation solely depicts a broad correlation between evaporation ratio and the aridity index. Consequently, to address this limitation, Budyko (1974), Fu (1981), and Yang et al. (2008) introduced empirical equations for estimating actual evaporation within the Budyko framework. These equations are presented as follows:

$$\frac{AET}{P} = \left\{\frac{PET}{P}\left[1 - \exp\left(-\frac{PET}{P}\right)\right]\tanh\left(1/\frac{PET}{P}\right)\right\}^{0.5} \tag{20}$$

$$\frac{AET}{P} = 1 + \frac{PET}{P} - \left[1 + \left(\frac{PET}{P}\right)^{w}\right]^{\frac{1}{w}} \tag{21}$$

$$\frac{AET}{P} = \left[1 + \left(\frac{PET}{P}\right)^{\alpha}\right]^{-\frac{1}{\alpha}} \tag{22}$$

In Fu's equation, the parameter 'w' represents catchment characteristics related to vegetation type, water storage, relative infiltration capacity hydraulics, and topography (Fu 1981; Padrón et al. 2017). The default value for 'w' in the Budyko framework is commonly set to 2.6 (); Li et al. 2013; Greve et al. 2016; Gan et al. 2021however, a value of 2 for 'w' as it aligned better with other equations employed in the Budyko analysis was utilized.

In addition, the parameter 'α' in Yang et al. (2008) equation signifies the characteristics of the basin landscape, primarily associated with soil, topography, and vegetation (Yang et al. 2008; Xu et al. 2014). There is a relationship between Fu's and the Choudhury–Yang equation, where 'w' is correlated with 'α' through the equation $w = \alpha + 0.72$. Both parameters are influenced by catchment characteristics, such as slope, soil texture, and vegetation (Gan et al. 2021; Xu et al. 2014; Yang et al. 2009). Therefore, in this study, the parameter $\alpha = 1.5$ based on this relationship was used.

In this study, a decomposition method proposed by Wang and Hejazi (2011) was employed to separate and quantify

the respective impacts of land cover change and climate variability on runoff. This method operates on the assumption that, in the absence of land cover land use activities the aridity index shifts to a different range solely due to climate change. Similarly, the evaporative ratio also undergoes a shift but continues to adhere to the same Budyko curve (Krajewski et al. 2021). Therefore, the alteration in Wami River runoff attributed to land cover change land use can be expressed using the following equation:

$$\Delta Q_{hum} = P_2\left(\frac{AET\prime_2}{P_2} - \frac{AET_2}{P_2}\right) \tag{23}$$

where P_2 is the average annual precipitation in the post-transformation period, AET'_2 is the annual AET in the post-transformation period estimated by the Budyko curves, AET_2 is the average annual AET post-transformation.

Analytical approach *Climate elasticity*: The impact of climate on river runoff can be evaluated through the climate elasticity method introduced by Schaake, (1990). This method examines how changes in precipitation and PET, correspond to changes in runoff on a proportional basis (Krajewski et al. 2021). The climate elasticity method is given by the following formula:

$$\Delta Q_{clim} = \left(\varepsilon P\frac{\Delta P}{\overline{P}} + \frac{\Delta PET}{\overline{P}}\right)\overline{Q}\# \tag{24}$$

whereby εPandεPET indicate the elasticity coefficient of runoff concerning precipitation and potential evapotranspiration, respectively, $\overline{P}$ is the long-term average annual precipitation, ΔP is the total change in precipitation, $\overline{Q}$ is the long-term average annual runoff and ΔPET is the total change in potential evapotranspiration (Mo et al. 2021). In this context, the Budyko approach provides the elasticity coefficient of runoff concerning precipitation and is indicated as the aridity index ($\phi = \frac{PET}{P}$)Dey and Mishra 2017; Arora 2002) as follows:

$$\varepsilon P = 1 + \frac{\varphi \mathrm{F}'(\varphi)}{1-F(\varphi)}\# \tag{25}$$

and

$$\varepsilon P + \varepsilon PET = 1\# \tag{26}$$

whereby F' is a derivative of the Budyko equations.

Hydrological sensitivity method: Changes in precipitation and PET have the potential to alter the water balance within the catchment. Therefore, this alteration can be assessed through the hydrological sensitivity method, which examines the changes in mean runoff relative to changes in mean annual precipitation (P), and PET (Li et al. 2007; Zuo et al. 2014).

The hydrological sensitivity method proposed by Dey and Mishra, (2017), provides insights to identify the change in mean runoff attributed to climate variability. The formula is as follows:

$$\Delta Q_{clim} = \frac{\partial Q}{\partial P}\Delta P + \frac{\partial Q}{\partial PET}\Delta PET\# \tag{27}$$

whereby ΔQ_{clim}, ΔP and ΔPET indicating changes in runoff due to climate variability, change in precipitation, and change in potential evapotranspiration, respectively (Jiang et al. 2011). $\frac{\partial Q}{\partial \mathrm{P}}$ and $\frac{\partial Q}{\partial \mathrm{PET}}$ illustrates the coefficients of sensitivity of runoff to precipitation and potential evapotranspiration, respectively (Li et al. 2007). It can be written as follows:

$$\frac{\partial Q}{\partial P} = \frac{1+2\phi+3\omega\phi}{(1+\phi+\omega\phi^2)^2}\# \tag{28}$$

$$\frac{\partial Q}{\partial PET} = -\frac{1+2\omega\phi}{(1+\phi+\omega\phi^2)^2}\# \tag{29}$$

where ϕ is the aridity index (PET/P) and ω is the plant-available water coefficient, whereby a change in the mean runoff may result from climate variability or land cover change based on the following equation:

$$\Delta Q = \Delta Q_{clim} + \Delta Q_{hum} \tag{30}$$

where ΔQ describes the change in the mean annual runoff between two periods and $\Delta Q_{clim} and \Delta Q_{hum}$ are the changes in the mean annual runoff due to climate variability and land use/cover, respectively (Chen et al. 2013). A change in the mean annual runoff can be computed as follows:

$$\Delta Q = \Delta Q_{obs1} - \Delta Q_{obs2} \tag{31}$$

where ΔQ_{obs1} is the average runoff in the pre-transformation period, and ΔQ_{obs2} is the average runoff in the post-transformation period. Then, the relative contribution of climate variability and land use/cover to runoff changes can be expressed as follows:

$$\Delta Q_{clim\%} = \frac{\Delta Q_{clim}}{\Delta Q} \times 100 \tag{32}$$

$$\Delta Q_{hum\%} = \frac{\Delta Q_{hum}}{\Delta Q} \times 100 \tag{33}$$

where $\Delta Q_{clim\%}$ and $\Delta Q_{hum\%}$ are the percentage contribution of climate variability and land use/cover, respectively, to runoff changes in the Wami river catchment.

Results

Spatiotemporal and the impact of land use and land cover

Classification accuracy

The accuracy assessment for our classification process gave the output of 76%, 81.2%, 85.4% and 85.83% for overall accuracy for 1991, 2001, 2011, and 2021 classification, while for Kappa statistics, the results were 72%, 78.5%, 83.7% and 84.2%, respectively, to the other accuracy, as shown in the table below.

Years	LU/LC	Producer accuracy	User accuracy	Overall accuracy	Kappa
1991	Built-Up	95.27897	91.73554	**75.93**	**72.65**
	Bare Land	98.43137	86.85121		
	Bush Land	85.5	51.12108		
	Agriculture	69.26148	87.40554		
	Woodland	71.14914	72.93233		
	Wetland	79.41176	81.46552		
	Forest	61.08597	89.701		

Years	LU/LC	Producer accuracy	User accuracy	Overall accuracy	Kappa
2001	Built-Up	92.90323	83.96501	**81.2**	**78.59**
	Bare Land	94.23077	84.12017		
	Bush Land	69.62264	83.86364		
	Agriculture	82.35294	78.53659		
	Woodland	72.52525	77.37069		
	Wetland	80.26316	84.13793		
	Forest	91.97531	80.75881		
2011	Built-Up	91.01124	83.96501	**85.47**	**83.76**
	Bare Land	89.9705	84.12017		
	Bush Land	83.28076	83.86364		
	Agriculture	82.44444	78.53659		
	Woodland	75.18987	77.37069		
	Wetland	95.9799	84.13793		
	Forest	89.0411	80.75881		
2021	Built-Up	94.78827	90.37267	**85.83**	**84.23**
	Bare Land	89.05109	93.84615		
	Bush Land	89.74359	89.3617		
	Agriculture	89.67254	91.75258		
	Woodland	71.2766	86.17363		
	Wetland	84.84848	88.11189		
	Forest	92.27642	73.7013		

LULC change in the Wami river catchment Through Landsat images between the years 1991 to 2021, managed to understand the existing LULC scenario of the Wami river catchment over a period of 30 years, which we obtained through the classification process. A total of seven major LULC classes were identified within the catchment area. These classes include built-up, wetlands, bare land, bushland, woodland, agricultural, and forests (Fig. 3).

The results derived from the classification between 1991 and 2021 years show that anthropogenic actions such as LULC are the major factor of alteration within the catchment (Fig. 4). Thus, in 1991, the catchment had a total area of 41,073 km^2 with bushlands being the most dominant LU/LC category, covering 58% of the total area. Agriculture and woodland were the second and third most dominant categories, covering 19.2% and 15% of the total area, respectively. In 2001, changes in the distribution of LU/LC categories were observed. Bushland retained its dominance, encompassing 53.7% of the entire area, agriculture (25.2%) became the second, followed by woodland (14.3%) as indicated in Table A.4 in supplementary material. In 2011, agriculture shows growth of almost 20%, covering 38.4% of the entire catchment. Despite bushland maintaining its position as the most prominent category, covering 49% of the entire catchment, woodland emerged as the third most dominant category, accounting for 7.9% of the overall land. In 2021, notable alterations occurred in the distribution of LULC within the catchment area. The built-up experienced a remarkable surge, escalating from 0.8% in 2011 to 4.2% in 2021, making it the fourth most dominant category, while agriculture became the most dominant category covering 48.8%, followed by bushland (38.3%). Therefore, agricultural expansions, charcoal production, and built-up area expansion are the main driving factors of Land use/cover change. The deterioration of vegetation cover (forest, woodland, and bushland), increasing of agricultural land and settlement land cover may increase the deterioration of natural ecosystem hence stakeholders' intervention is requiring minimizing the potential impacts.

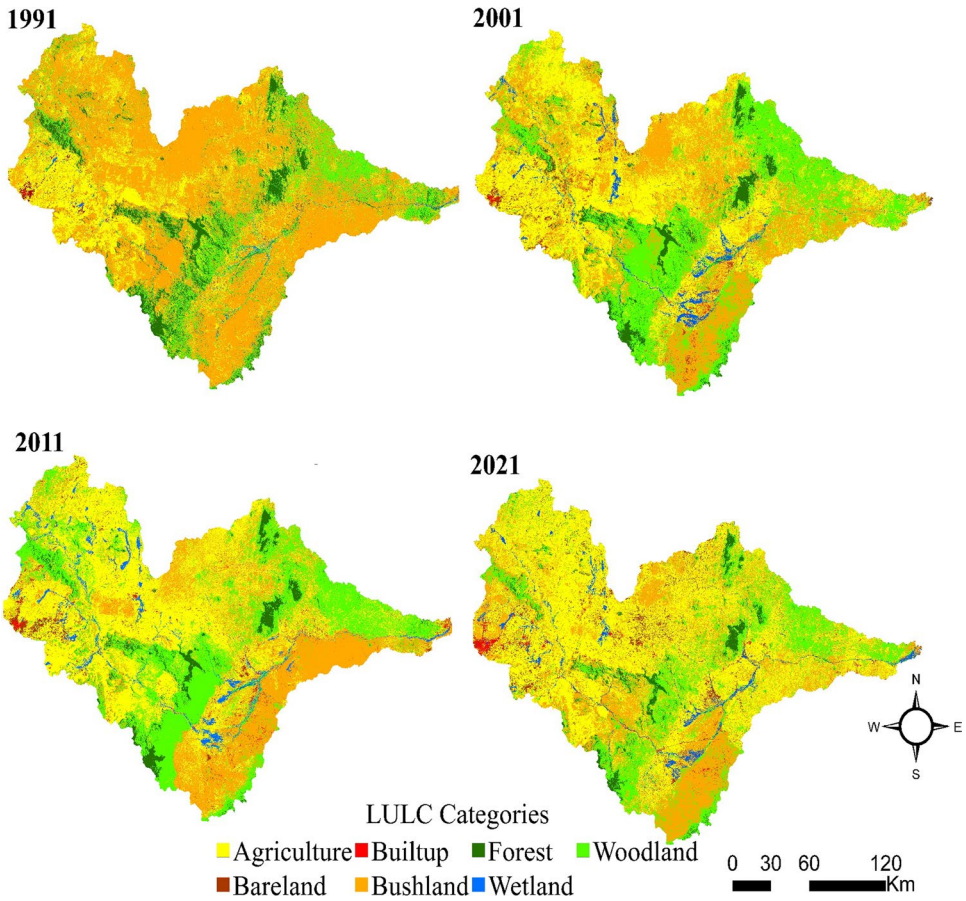

Fig. 3 LULC of Wami river catchment from 1991 to 2021

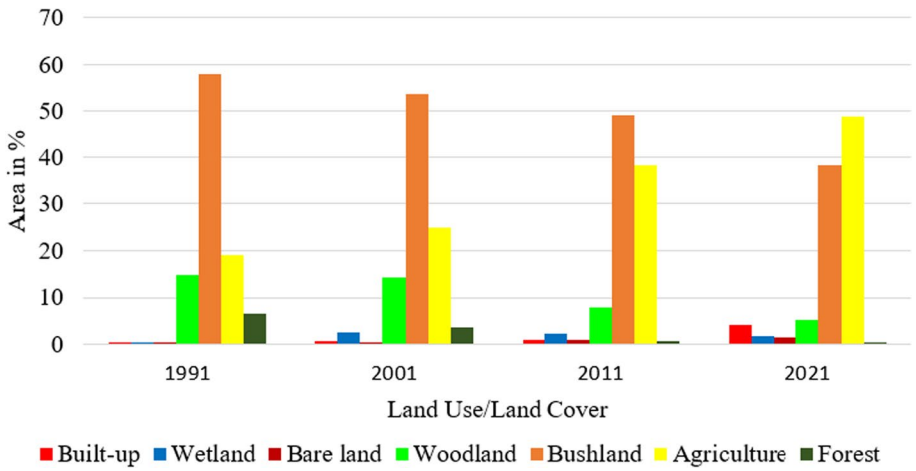

Fig. 4 LULC graph for 1991, 2001, 2011, and 2021 at the Wami River sub-basin

Comparison of observed and ERA5-Land precipitation A point-to-pixel approach was used to compare only monthly observed rain gauges and ERA5-Land precipitation data to eliminate uncertainties during interpolation. The results, shown in Table A.5 as shown in supplementary material, there was a moderate to strong correlation observed between the observed precipitation and ERA5-Land data set. The Pearson correlation coefficient ranged from 0.52 to 0.75, indicating a significant relationship between the two data sets (Moriasi et al. 2007; Mararakanye et al. 2020). In addition, MAE magnitude ranges from 30.49 to 45.35, and RMSE is from 47.84 to 63.89. PBIAS values range from – 42.10 to 60.45, with an average value of 1.40, hence this indicated a tendency of underestimation of some stations and overestimation for others. The ERA5-Land precipitation performs moderately well against rain gauges at the differ-

ent weather stations, with the highest correlation and lowest error at the Kongwa station and the lowest correlation and highest error at the Mandera station (Table A.6). The average values of the statistical measure across all stations in the entire catchment indicate the moderate performance of the ERA5-Land precipitation data.

Mann–Kendall trend test of annual ERA5-Land data The Mann–Kendall (MK) test was used to analyse annual climatological and hydrological variables from 1960 to 2021 to identify long-term trends within the catchment. The results of the analysis (as shown in Table A.6 in supplementary material) suggests that the annual temperature has been increasing significantly at a rate of 0.02 ^{0}C per year. Precipitation and AET, on the other hand, show negative trends with decreasing rates of 2.2 mm per year and 2.4 mm per year, respectively. Furthermore, PET displays a positive trend, albeit not statistically significant, with an annual increase of 5.19 mm. On the other hand, runoff demonstrates a decreasing trend with a decline rate of 0.30 mm per year, which similarly, lacks statistical significance.

Identified change point The mean annual runoff in the pre-transformation and post-transformation changes due to LULC is 47 mm/year and 38 mm/year, respectively. When comparing the two changes period, it is evident that the Wami River runoff undergoes a decrease of 9 mm per year (equivalent to a 19% reduction) within the Wami river catchment (Table A.7 in supplementary). The mean annual precipitation during the pre-transformation and post-transformation is 1094 mm per year and 997 mm per year, respectively, which shows a minimal decrease of 97 mm per year (8.9%). The mean PET during the pre- and post-transformations is 4786 mm per year and 5032 mm per year, respectively, which indicates a yearly increase of 246 mm (5%). In addition, the average annual air temperature experienced a shift in the pre-and post-transformation phases, with values of 22.8 °C per year and 23.4 °C per year, respectively. This indicates an increase of 0.6 °C per year (equivalent to 2.6% of the long-term average). Furthermore, the mean annual AET within the Wami river catchment experienced changes as well. In the pre-transformation period, it indicated 1034 mm per year, whereas in the post-transformation period, it decreased to 941 mm per year, signifying a decline of 93 mm per year (8.9%). Consequently, during the post-transformation period (1993–2021), the annual air temperature rose by 0.6 °C (which accounts for 2.6% of the long-term average), while the overall annual precipitation decreased by 107 mm (9.7% of the long-term average). This alteration resulted in a reduction of 9 mm (19%) in the annual runoff within the catchment.

Results from the conceptual approach *Results from tommer and schilling framework*: To assess the impact of climate change and anthropogenic actions within the catchment, both the pre- and post-transformations periods were evaluated. Following the conceptual approach proposed by Tomer and Schilling, (Sneyers 1975), the energy excess (E_{ex}) augmented from 0.78 to 0.81, while the water excess (P_{ex}) diminished from 0.06 to 0.05. Based on the findings presented in Table A.3, it can be concluded that changes in Wami River runoff are primarily influenced by shifts in climatic factors, and minor by changes in land cover change. However, the methods give the general information as to either the variation in runoff is due to land management or climate variability.

Budyko decomposition: Fig. 5 illustrates the spatial distribution of the catchment area in Budyko space. The evaporation ratio, represented by AET/P, reflects the relationship

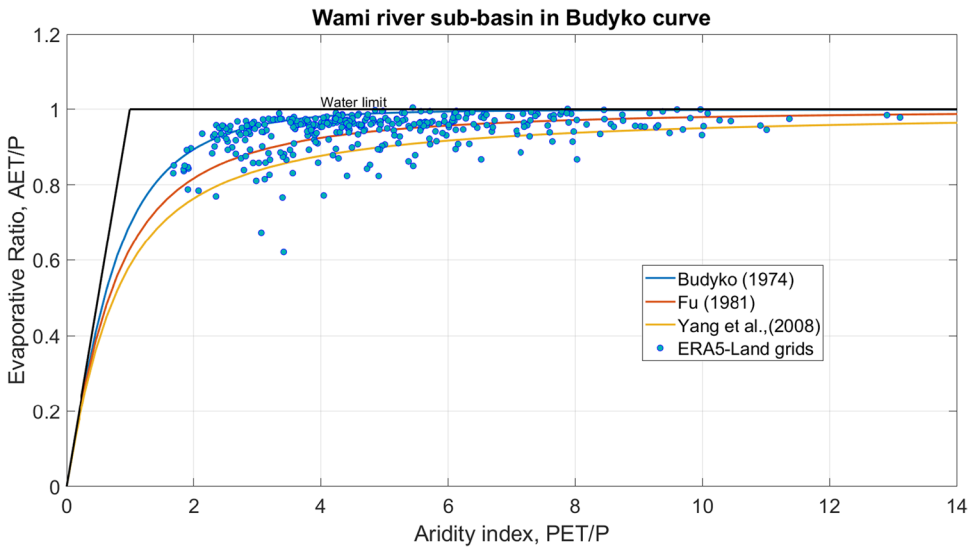

Fig. 5 Established Budyko curves for the Wami river catchment and indicate the distribution of catchments in Budyko space

between actual evaporation and precipitation. On the other hand, the aridity index (ϕ), is a function of potential evaporation and precipitation (PET/P), defined by Budyko (1974). The ϕ is used to classify climate zones, such as hyper-arid ($\phi > 20$), arid ($5 < \phi \leq 20$), semiarid ($2 < \phi \leq 5$), dry sub-humid ($1.5 < \phi \leq 2$), and humid ($\phi < 1.5$) (Ponce et al. 2000; Cherlet et al. 2018).

The Budyko curves based on the equations proposed by Budyko (1974), Fu (1981), and Yang et al. (2008) were developed for the Wami river catchment. The findings revealed that a majority of the catchment's parts (represented by ER5-Land grids) are located in arid and semi-arid areas, while a small portion (2.9%) falls within the dry sub-humid zone in the Budyko space.

Due to the prevalence of arid a semi-arid condition in the catchments, characterized by elevated potential evaporation, limited precipitation, and evapotranspiration, it can be demonstrated that an increase in the aridity index is associated with a decrease in runoff within these areas (Fig. 6).

The impact of climate variability and LULC actions on runoff alteration was examined using three decomposition methods. The analysis of these equations revealed that climate factors played a primary role in the changes observed within the catchment, as indicated in Table 4. The decomposing proposed by Budyko (1974) indicated that reduction in runoff (averaging 9.0917 mm) was primarily influenced by climate variability (100%). Further analysis conducted using Fu (1981) and Yang et al. (2008) suggested that climate variability accounted for approximately 99.3% and 99.7% of the runoff reduction in the Wami river catchment, while land cover change contributed only 0.7% and 0.3%, respectively.

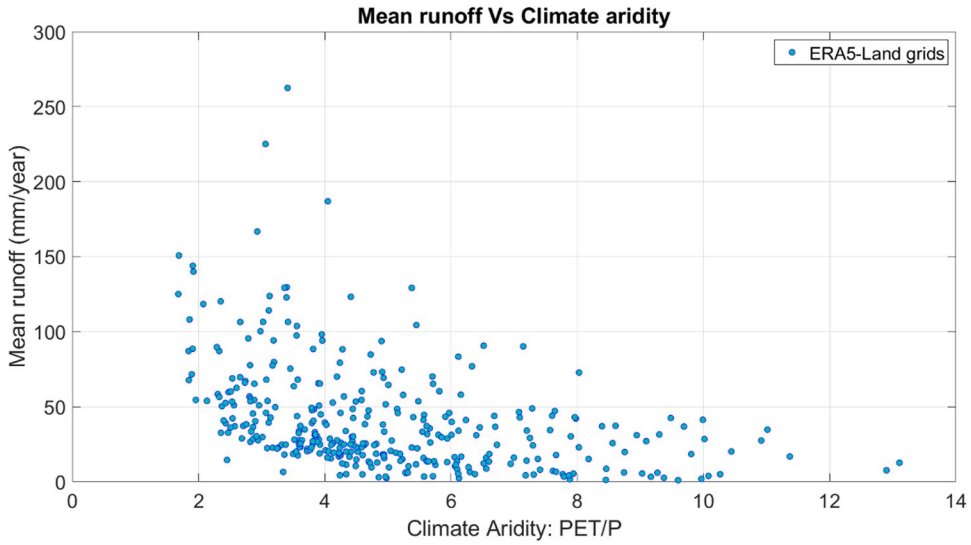

Fig. 6 Mean runoff and climate aridity in the Wami river catchment

Table 4 Results of Budyko decomposition

Budyko decomposition	Standard Error	ΔQ (mm)	ΔQ^H (mm)	ΔQ^C (mm)	ΔQ^H (%)	ΔQ^C (%)
Budyko (1974)	0.0102	– 9.0917	0.0198	– 9.1115	0	100
Yang et al. (2008)	0.0071	– 9.0917	– 0.0247	– 9.0669	0.3	99.7
Fu (1981)	0.0093	– 9.0917	– 0.0673	– 9.0243	0.7	99.3

Table 5 Computed parameters and contribution of climate elasticity and hydrological sensitivity methods

		σP	σPET	ΔQ (mm)	ΔQ^H (mm)	ΔQ^C (mm)	ΔQ^H (%)	ΔQ^C (%)
Climate Elasticity	Budyko (Budyko 1974)	0.08	0.92	– 9.0917	– 7.2	– 1.9	79.3	20.7
	Yang et al., (2008)	0.02	0.98	– 9.0917	– 1.05	– 8.04	11.6	88.4
	Fu (Fu 1981)	– 1.63	2.63	– 9.0917	– 1.99	– 7.10	21.9	78.1
Hydrological Sensitivity	Parameters acc. To Li et al. (Li et al. 2007)	β	γ	ΔG (mm)	ΔG^H (mm)	ΔG^C (mm)	ΔG^H (%)	ΔG^C (%)
		0.027	– 0.014	– 9.0917	– 2.8	– 6.3	30.6	69.4

Results from an analytical approach *Climate elasticity*: The climate elasticity approach was used to determine the climate elasticity coefficients of Wami River runoff by considering the ERA5-Land data from the years 1960–2021. The results, according to the Fu (1981), and Yang et al. (2008) equations indicate that climate variability contributed to the reduction of the Wami River runoff by 78.1% and 88.3%, while land cover change such as LULC accounts for 21.9% and 11.6%, respectively. However, the Budyko equation indicated that land use land change as the dominant factor affecting river runoff by 79.3%, while climate variability contributed by only 20.7% in the river runoff reduction.

Hydrologic sensitivity: The hydrologic sensitivity equation developed by Li et al. (2007) was used to quantify the sensitivity of climate variability and land cover change on Wami River runoff. In the catchment, the average annual precipitation experienced a decrease from 1094 mm per year in the pre-transformation period to 997 mm per year after post-transformation. Conversely, average PET displayed an upward trend of 5%. The influence of climate variability on runoff was assessed by considering the annual average of precipitation and PET. The findings presented in Table 5, revealed that climate variability accounted for 69.4% of the change in annual runoff, while land cover change contributed to 30% of changes. It is worth noting that the impact of climate variability and land cover on runoff in the catchment differed significantly during the period of transformation. Therefore, the primary factor contributed to the decline of river runoff is climate variability.

Discussion

Land use and land cover change

The Wami river catchment economy is heavily relying on agriculture, leading to overuse of forest land, woodland, and bushland for farming purposes to support the rapidly growing population. This has caused a decline in forest resources, negatively impacting the basin's ecosystem services. Over the past 30 years, agricultural land has grown at a rate of 48%, while settlements have grown at a rate of 4.25% (Table A.4 in supplementary material). Forest vegetation within the catchment has rapidly decreased, and wetlands have also experienced a similar trend. Almost 50% of water bodies have been lost due to environmental modification and unwise water usage in the last 30 years. Due to the agriculture sector's predominant role in the catchment's economy, agricultural water usage constitutes portion of the overall water consumption. The expansion of cultivated areas and agricultural irrigation practices are key factors contributing to this trend within the catchment. Therefore, deterioration of vegetation cover (forest, woodland, and bushland) and the increasing coverage of agriculture activities and settlement land may cause to further decline of natural ecosystems. Henceforth, the implementation of a nature-based solution is significantly important to reverse the natural ecosystem around the catchment.

The study classification faced many misclassification pixels for natural vegetation, such as woodland, and bushland, which were prone to errors due to gradual differences in reflectance characteristics, although post-classification comparisons were mostly consistent and conformed to historical maps. However, cropland, water, and bare land were less prone to errors due to strong spectral changes. In addition, the study faced a lot of challenges in ground truthing in dense forest land.

The results in this paper, along with similar results in Jamila Ngondo et al. (2021), who provide the information Wami–Ruvu river basin natural areas, including forests and grasslands, were intensively converted into agricultural land from 1990 to 2018; furthermore, these changes are anticipated to continue towards 2036, This LULC pattern is main influenced by economic forces that reinforce anthropogenic activities on LULC change in the basin.

Nobert and Jeremiah (2012) observed an increase in agriculture by 42.53% from 1990 to 2018 which resulted in the degradation of grasslands and wetlands. In their study, they found that most wetlands in some areas of the basin were converted into agricultural areas for rice and maize. In general, this change highlights the increasing demand for food production resulting from the increasing population pressure. Twisa et al. (2019) studied land use/land changes in the Wami-river basin and found that the changes in the basin are influenced by population growth which results in the conversion of natural vegetation into settlements land and agricultural fields as observed in the classified image.

Periodic (annually) Land use/cover Monitoring for the sub-basin and whole basin in the Wami-river are required for current and past change detection of LULC parameters to determine the rate and condition of their change this is of very high importance, because the basin experience such an alarming situation of degradation of forests and water, due to rapid expansion of agricultural activities. Meanwhile, periodic evaluation of the rate of reduction is lacking for a proper understanding of their impacts, particularly on land use and land cover change, biodiversity losses, and climate change. Therefore, time-based studies for the prediction of LULCC consequences on water resources and loss of biodiversity are vital for decision-making towards the sustainability of water resources and filling the time-based gap of LULCC information. Further to the specific strategies, there is a need also to build broad and increased public awareness on the impact of LULC due to the increase of anthropogenic alteration on the basin land. This strategy can be applied to other basins globally.

The trend of temperature and precipitation

The findings from our study indicated that the reduction of runoff in the Wami river catchment during the post-transformation period was primarily influenced by climate variability, although both climate variability and LULC action played a role in shaping changes within the catchment. The Mann–Kendall trend test was employed to analyse temperature patterns within the catchment, the result showed a significantly increasing trend with an average rate of 0.02 °C per year (equivalent to 1.22 °C per 61 years) (Fig A.2). This rate is higher than the global average temperature increases of 0.0074 °C per year (or 0.74 °C per century) as reported by Funk et al. (2012); and Mahmood et al. (2019). In a study conducted by Collins (2011), it was observed that Africa experience a faster temperature increase compared to other regions, with a rate of 0.016 °C per year. Considering this, if the temperature trend in the catchment follows a similar pattern, it suggested that the catchment could potentially face a temperature rise of approximately 2 °C over the next century.

Furthermore, as highlighted in the Sixth Assessment Report of the Intergovernmental Panel on Climate Change (IPCC), the rising concentration of greenhouse gases has emerged as the primary driver of the global warming (Pörtner et al. 2022). Despite Africa's relatively low contribution of less than 4% to the global average (around 1 million metric tons, but the content has been disproportionately impacted by global warming. Consequently, the temperature increase observed in the Wami river catchment could pose serious challenge to water resources, agriculture activities, and the occurrence of floods and droughts.

Therefore, this study reveals a decline in annual precipitation between 1960 to 2021, characterized by a strong downward trend of 2.21 mm per year. Although the statistical significance at 95% confidence level is not attained (Fig. A.6), the cumulative reduction in precipitation over the 61 year period amounts to 134.81 mm. This decline in precipitation within the catchment attributed by various factors, including changes in air temperature, and vegetation decline. If this trend continues in the future, it may have significant implications for the sustainability of surface water resources and groundwater recharge. This concern is particularly relevant as the population of catchment continue to increase, leading to a further rise in land cover change.

Identified step change

The Mann–Kendall–Sneyers test was used to identify the point of step change in the annual runoff series from 1960 to 2021. As a result, the period from 1960–1992 was considered the natural period, characterized by minimal influence from anthropogenic activities on water resources in the catchment. Subsequently, the period from 1993 to 2021 was designated as a post-transformation period, during which both climate and anthropogenic actions contribute to perturbations in river runoff. Mean annual precipitation, AET, runoff and PET were assessed in pre- and post-transformation period, as shown in Table A.8. It was observed that in the post-transformation period, PET experienced a 5% increase, runoff exhibited a substantial decrease by 19%, while both precipitation and AET showed a decrease of 9%. Therefore, the continuous decrease in precipitation and runoff will have a significant impact on the river health. This decline in water availability will not only affect the ecological aspects but also have far-reaching consequence on the socio-economic aspects of the catchment. Rain-fed agriculture, which serves as the primary economic source in the basin, will be several affected, leading to a decline in agricultural productivity and potential economic losses. In addition, the local population will continue to face challenge of limited access to clean and safe water for both domestic and industrial purpose. Currently, people and economic activities around the catchment are already grappling with water scarcity issues, prompting the government to explore alternative such as groundwater extraction to compensate for the decreasing surface water availability.

Effect of climate change and LULC.

In a research conducted by Xue et al. (2017), it was described that arid river catchment encounter severe water issues. Similarly, in the case of the Wami river catchment, where a majority of parts are arid and semi-arid, as illustrated in Fig. 3. It can be inferred that the notable increase in water issues, coupled with rising temperature, is likely to have resulted in high PET, which ultimately leading to persistent of drought condition in the study area. Furthermore, building upon the previous findings, it is worth noting that climate aridity plays a significant role in shaping the mean annual runoff in the catchment, as indicated in Fig. 4. This exacerbates the existing challenges faced by the social and economic sectors, particularly in terms of limited water access during the dry period, as highlighted by Nachilongo (2021). The combined impact of water scarcity, arid conditions, and reduced runoff further compounds the difficulties faced by the Wami river catchment, necessitating a comprehensive approach to address these pressing issues.

Furthermore, in our study, decomposition methods, climate elasticity, and hydrological sensitivity methods were used. These approaches allowed to assess the influence of climate change and alteration of water resources, particularly river runoff within the catchment area. According to the findings, Yang et al. (2008), Fu's (1981), and Budyko's (1974) equations demonstrated that climate change is a

significant dominant affecting runoff. However, it is worth noting that Budyko's (1974) equation does not account for changes in catchment properties, resulting in all runoff changes being solely driven by climatic variables, such as PET and P. In addition, the calculated standard error for this equation was relatively high compared to the others. On the other hand, both Yang et al. (2008) and Fu (1981) equations incorporate a term that consider changes due to land cover land use and climate properties. As result, the changes in runoff from these equations also reflects the contribution of land cover change.

Conclusion

The study found that both climate variability and land use land cover change (LULC) have markedly influenced the reduction of runoff in Tanzania's Wami river catchment. Specifically, the climate variability has significantly influenced to the decrease in river runoff, precipitation, and actual evapotranspiration. Concurrently, there was an increase in temperature and potential evapotranspiration during the post-transformation period compared to the period preceding land cover change. These findings showcase the complex interplay between climate variability and land cover operations in the Wami river catchment.

The Yang (Yang et al. 2008) and Fu (1981) showed that Budyko decomposition exhibited reductions in river runoff within the catchment by 99.7%, 99.3%, respectively, climate elasticity by 88.3%, 78.1%, respectively, and hydrological sensitivity by 66.4%. These findings underscore the substantial contribution of climate variability to the reduction in river runoff. Conversely, the land cover change activities contributed to the reduction by 0.3%, 0.7%, 11.6%, 21.9% and 30.6%, respectively, further emphasizing the multifaceted factors influencing the hydrological dynamics of the area. Thus, while the land cover change activities contribution was relatively low, the Wami river catchment displayed heightened sensitivity to climate variability. This observation underscores the necessity for implementing effective climate adaptation strategies, with particular emphasis on nature-based solutions.

However, this study is constrained by its reliance solely on long-term reanalysis data (ERA5-Land) due to the insufficient availability of observed rainfall data. Consequently, in future research study, it is crucial to incorporate observed long-term time series data to enhance the comprehensiveness of the analysis. This will contribute to a more robust understanding of the complex interactions between climate variables. In turn, would improve the overall reliability of the study's findings and deepen our insights into the climate variability and land cover change dynamics of the study area.

Supplementary Information The online version contains supplementary material available at https://doi.org/10.1007/s12665-023-11383-3.

Author contribution All authors contributed to the study conception and design. Material preparation and data collection was performed by Christossy Lalika, Data analysis was performed by Christossy Lalika and Aziz Ul Haq Mujahid. The first draft of the manuscript was written by Christossy Lalika and reviewed by Aziz Ul Haq Mujahid and Makarius C.S Lalika. All authors read and approved the final manuscript.

Funding The authors declare that no funds, grants, or other support we received during the preparation of this manuscript.

Data availability The data presented in this study are available on request from the corresponding authors.

Declarations

Conflict of interest The authors have no relevant financial or non-financial interest to disclose.

References

Alexandersson H (1986) A Homogeneity Test Applied to Precipitation Data. J Climatol 6:661

Aminikhanghahi S, Cook DJ (2017) A Survey of Methods for Time Series Change Point Detection. Knowl Inf Syst 51:339

Arora VK (2002) The Use of the Aridity Index to Assess Climate Change Effect on Annual Runoff. J Hydrol 265:164

Atta-ur-Rahman and M. Dawood, *Spatio-Statistical Analysis of Temperature Fluctuation Using Mann–Kendall and Sen's Slope Approach*, Clim Dyn **48**, 783 (2017).

Ayehu GT, T. Tadesse, B. Gessesse, and T. Dinku, Validation of New Satellite Rainfall Products over the Upper Blue Nile Basin, Ethiopia, preprint, Others (Wind, Precipitation, Temperature, etc.)/Remote Sensing/Validation and Intercomparisons, 2017.

Balist J, Malekmohammadi B, Jafari HR, Nohegar A, Geneletti D (2021) Detecting Land Use and Climate Impacts on Water Yield Ecosystem Service in Arid and Semi-Arid Areas. A Study in Sirvan River Basin-Iran, Appl Water Sci 12:4

Belgiu M, Drăguţ L (2016) Random Forest in Remote Sensing: A Review of Applications and Future Directions. ISPRS J Photogramm Remote Sens 114:24

Budyko MI (1948) *Evaporation under Natural Conditions, Gidrometeorizdat, Leningrad*, English Translation by IPST, Jerusalem 635

Budyko MI (1974) *Climate and Life* (Academic Press, New York)

Buishand TA (1982) Some Methods for Testing the Homogeneity of Rainfall Records. J Hydrol 58:11

Chen Z, Chen Y, Li B (2013) Quantifying the effects of climate variability and human activities on runoff for Kaidu River Basin in arid region of Northwest China. Theor Appl Climatol 111:537

Cherlet M, Hutchinson C, J. Reynolds, J. Hill, S. Sommer, and M. G. Von, *World Atlas of Desertification*, https://doi.org/10.2760/06292.

Chiaravalloti F, Caloiero T, Coscarelli R (2022) The Long-Term ERA5 Data Series for Trend Analysis of Rainfall in Italy. Hydrology 9:2

Cohen J (1960) A Coefficient of Agreement for Nominal Scales. Educ Psychol Measur 20:37

Collins JM (2011) Temperature Variability over Africa. J Clim 24:3649

da Silva RM, Santos CAG, Moreira M, Corte-Real J, Silva VCL, Medeiros IC (2015) Rainfall and River Flow Trends Using

Mann-Kendall and Sen's Slope Estimator Statistical Tests in the Cobres River Basin. Nat Hazards 77:1205
Dey P, Mishra A (2017) Separating the impacts of climate change and human activities on streamflow: a review of methodologies and critical assumptions. J Hydrol 548:278
Dhawan P, Dalla Torre D, Zanfei A Menapace A, Larcher M, Righetti M (2023) Assessment of ERA5-Land Data in Medium-Term Drinking Water Demand Modelling with Deep Learning, Water 15:8
Dietterich TG (2000) *Ensemble Methods in Machine Learning*, in (Springer), pp. 1–15
Ervinia A, J. Huang, and Z. Zhang, *Assessing the Specific Impacts of Climate Variability and Human Activities on Annual Runoff Dynamics in a Southeast China Coastal Watershed*, WATER **9**, (2017).
Eyasmin F (2017) Perception of and Adaptive Capacities to Climate Change Adaptation Strategies and Their Effects on Rice Production: A Case of Pabna District. Bangladesh, JHER 3:8
Fu BP (1981) On the Calculation of the Evaporation from Land Surface. Sci Atmos Sin 5:23
Funk C, J. Rowland, G. Eilerts, A. Adoum, and L. White, *A Climate Trend Analysis of Chad*, FEWSNET/US Geological Survey Fact Sheet **3070**, (2012).
Gan G, Liu Y, Sun G (2021) Understanding Interactions among Climate, Water, and Vegetation with the Budyko Framework. Earth Sci Rev 212:103451
Gocic M, Trajkovic S (2013) Analysis of Changes in Meteorological Variables Using Mann-Kendall and Sen's Slope Estimator Statistical Tests in Serbia. Global Planet Change 100:172
Greve P, Gudmundsson L, Orlowsky B, Seneviratne SI (2016) A Two-Parameter Budyko Function to Represent Conditions under Which Evapotranspiration Exceeds Precipitation. Hydrol Earth Syst Sci 20:2195
Jiang S, Ren L, Yong B, Singh VP, Yang X, Yuan F (2011) Quantifying the Effects of Climate Variability and Human Activities on Runoff from the Laohahe Basin in Northern China Using Three Different Methods. Hydrol Process 25:2492
Kalugendo P, Sustainable Water Resources Management for Agricultural and Industrial Water Sectors–Participation of Stakeholders in the Water Resources Management and Development, Wami/Ruvu Basin Office, 2014.
Kanyabwoya D, Dar Water Crisis: End Inaction to Save Ruvu Basin - The Chanzo Initiative, https://thechanzo.com/2022/11/18/dar-water-crisis-end-inaction-to-save-ruvu-basin/
Kendall MG (1975) Rank Correlation Methods; Griffin: London, UK, 1975, Google Scholar
Kim Y, Kimball JS, Zhang K, Didan K, Velicogna I, McDonald KC (2014) Attribution of Divergent Northern Vegetation Growth Responses to Lengthening Non-Frozen Seasons Using Satellite Optical-NIR and Microwave Remote Sensing. Int J Remote Sens 35:3700
Krajewski A, Sikorska-Senoner AE, Hejduk L, Banasik K (2021) An Attempt to Decompose the Impact of Land Use and Climate Change on Annual Runoff in a Small Agricultural Catchment. Water Resour Manage 35:881
Lalika MCS, Meire P, Ngaga YM (2015) and L. Chang'a, Understanding Watershed Dynamics and Impacts of Climate Change and Variability in the Pangani River Basin, Tanzania, Ecohydrology & Hydrobiology 15:26
Lang J et al (2017) Investigating the Contribution of Shipping Emissions to Atmospheric PM2.5 Using a Combined Source Apportionment Approach, Environmental Pollution 229:557
Li L-J, Zhang L, Wang H, Wang J, Yang J-W, Jiang D-J, Li J-Y, Qin D-Y (2007) Assessing the Impact of Climate Variability and Human Activities on Streamflow from the Wuding River Basin in China. Hydrol Process 21:3485
Li D, Pan M, Cong Z, Zhang L, Wood E (2013) Vegetation Control on Water and Energy Balance within the Budyko Framework: VEGETATION CONTROL ON WATER AND ENERGY BALANCE. Water Resour Res 49:969
Liu P, Jiang Z, Li Y, Lan F, Sun Y, Yue X (2023) Quantitative Study on Improved Budyko-Based Separation of Climate and Ecological Restoration of Runoff and Sediment Yield in Nandong Underground River System. Water 15:7
Luhunga P (2018) Evaluation of the Impacts of Climate Variability on Rainfed Maize Production over the Wami-Ruvu Basin of Tanzania. Journal of Water and Climate Change 9:207
Mahmood R, Jia S, Zhu W (2019) Analysis of Climate Variability. Trends, and Prediction in the Most Active Parts of the Lake Chad Basin, Africa, Sci Rep 9:1
Mann HB (1945) Nonparametric Tests Against Trend. Econometrica 13:245
Mararakanye N, Le Roux JJ, Franke AC (2020) Using Satellite-Based Weather Data as Input to SWAT in a Data Poor Catchment. Physics and Chemistry of the Earth, Parts a/b/c 117:102871
Mo C, Ruan Y, Xiao X, Lan H, Jin J (2021) Impact of Climate Change and Human Activities on the Baseflow in a Typical Karst Basin. Southwest China, Ecological Indicators 126:107628
Mohammad L, Mondal I, Bandyopadhyay J, Pham QB, Nguyen XC, Dinh CD, Al-Quraishi AMF (2022) Assessment of Spatio-Temporal Trends of Satellite-Based Aerosol Optical Depth Using Mann-Kendall Test and Sen's Slope Estimator Model. Geomat Nat Haz Risk 13:1270
Moriasi D, Arnold J, Van Liew M, Bingner R, Harmel RD, Veith T (2007), *Model Evaluation Guidelines for Systematic Quantification of Accuracy in Watershed Simulations*, Transactions of the ASABE 50
Mulungu DMM, Mukama E (2022) Evaluation and Modelling of Accuracy of Satellite-Based CHIRPS Rainfall Data in Ruvu Subbasin, Tanzania. Model Earth Syst Environ
Muñoz-Sabater J et al (2021) ERA5-Land: A State-of-the-Art Global Reanalysis Dataset for Land Applications. Earth System Science Data 13:4349
Nachilongo H (2021) Tanzania: Water Rationing Kicks in As Shortage Bites in Dar Es Salaam, The Citizen
Nawaz M, Iqbal MF, Mahmood I (2021) Validation of CHIRPS Satellite-Based Precipitation Dataset over Pakistan. Atmos Res 248:105289
Ngondo J, Mango J, Liu R, Nobert J, Dubi A, Cheng H (2021) Land-Use and Land-Cover (LULC) Change Detection and the Implications for Coastal Water Resource Management in the Wami-Ruvu Basin. Tanzania, Sustainability 13:4092
Ngondo J, Mango J, Nobert J, Dubi A, Li X, Cheng H (2022) Hydrological Response of the Wami-Ruvu Basin to Land-Use and Land-Cover Changes and Its Impacts for the Future. Water 14:2
Nobert J, Jeremiah J (2012) Hydrological Response of Watershed Systems to Land Use/Cover Change. a Case of Wami River Basin. The Open Hydrology Journal 6
Nyikadzino B, Chitakira M, Muchuru S (2020) Rainfall and Runoff Trend Analysis in the Limpopo River Basin Using the Mann Kendall Statistic. Physics and Chemistry of the Earth, Parts a/b/c 117:102870
Padrón RS, Gudmundsson L, Greve P, Seneviratne SI (2017) Large-Scale Controls of the Surface Water Balance Over Land: Insights From a Systematic Review and Meta-Analysis. Water Resour Res 53:9659
Perera A, Ranasinghe T, Gunathilake M, Rathnayake U (2020) Comparison of Different Analyzing Techniques in Identifying Rainfall Trends for Colombo. Sri Lanka, Advances in Meteorology 2020:1

Ponce VM, Pandey RP, Ercan S (2000) Characterization of Drought across Climatic Spectrum. J Hydrol Eng 5:222

Pörtner H-O, Roberts DC, Adams H, C. Adler, P. Aldunce, E. Ali, R. A. Begum, R. Betts, R. B. Kerr, and R. Biesbroek, Climate Change 2022: Impacts, Adaptation and Vulnerability, IPCC Sixth Assessment Report (2022).

Roy S, Farzana K, Papia M, Hasan M (2015) Monitoring and Prediction of Land Use/Land Cover Change Using the Integration of Markov Chain Model and Cellular Automation in the Southeastern Tertiary Hilly Area of Bangladesh, International Journal of Sciences: Basic and Applied Research (IJSBAR) 24:4.

Rwanga SS, Ndambuki JM (2017) Accuracy Assessment of Land Use/Land Cover Classification Using Remote Sensing and GIS. IJG 08:611

Schaake JC (1990) From Climate to Flow., Climate Change and US Water Resources. 177

Sen PK (1968) Estimates of the Regression Coefficient Based on Kendall's Tau. J Am Stat Assoc 63:1379

Shao Z, Fu H, Li D, Altan O, Cheng T (2019) Remote Sensing Monitoring of Multi-Scale Watersheds Impermeability for Urban Hydrological Evaluation. Remote Sens Environ 232:111338

Sneyers R (1975) Sur I'analyse Statisque Des Series d'observations. WMO Tech, Note

Tomer MD, Schilling KE (2009) A Simple Approach to Distinguish Land-Use and Climate-Change Effects on Watershed Hydrology. J Hydrol 376:24

Twisa S, Buchroithner MF (2019) Land-Use and Land-Cover (LULC) Change Detection in Wami River Basin. Tanzania, Land 8:136

Wambura FJ, Ndomba PM, Kongo V, Tumbo SD (2015) Uncertainty of Runoff Projections under Changing Climate in Wami River Sub-Basin. Journal of Hydrology: Regional Studies 4:333

Wang D, Hejazi M (2011) Quantifying the Relative Contribution of the Climate and Direct Human Impacts on Mean Annual Streamflow in the Contiguous United States: CLIMATE AND DIRECT HUMAN IMPACTS ON STREAMFLOW, Water Resour. Res. 47

Xie W, Yi S, Leng C, Xia D, Li M, Zhong Z, Ye J (2022) The Evaluation of IMERG and ERA5-Land Daily Precipitation over China with Considering the Influence of Gauge Data Bias. Sci Rep 12:1

Xu X, Yang D, Yang H, Lei H (2014) Attribution Analysis Based on the Budyko Hypothesis for Detecting the Dominant Cause of Runoff Decline in Haihe Basin. J Hydrol 510:530

Xue L, Yang F, Yang C, Chen X, Zhang L, Chi Y, Yang G (2017) Identification of Potential Impacts of Climate Change and Anthropogenic Activities on Streamflow Alterations in the Tarim River Basin. China, Sci Rep 7:1

Yang H, Yang D, Lei Z, Sun F (2008) New Analytical Derivation of the Mean Annual Water-Energy Balance Equation: DERIVING A WATER ENERGY BALANCE EQUATION. Water Resour. Res. 44

Yang D, Shao W, Yeh PJ-F, Yang H, Kanae S, Oki T (2009) Impact of Vegetation Coverage on Regional Water Balance in the Nonhumid Regions of China, Water Resources Research 45

Zuo D, Xu Z, Wu W, Zhao J, Zhao F (2014) Identification of Streamflow Response to Climate Change and Human Activities in the Wei River Basin. China, Water Resour Manage 28:833